**Registry No.** ADH, 9031-72-5; cyclohexanol, 108-93-0.

REFERENCES

Bosron, W. F., Li, T.-K., & Vallee, B. L. (1979) *Biochem. Biophys. Res. Commun. 91*, 1549-1555.

Bosron, W. F., Li, T.-K., & Vallee, B. L. (1980) *Proc. Natl. Acad. Sci. U.S.A. 77*, 5784-5788.

Bosron, W. F., Magnes, L. J., & Li, T.-K. (1983) *Biochemistry 22*, 1852-1857.

Deetz, J. S., Luehr, C. A., & Vallee, B. L. (1984) *Biochemistry 23*, 6822-6828.

Fong, W. P., & Keung, W. M. (1987) *Biochemistry* (preceding paper in this issue).

Harada, S., Misawa, S., Agarwal, D. P., & Goedde, W. (1980) *Am. J. Hum. Genet. 32*, 8-15.

Hempel, J., Holmquist, B., Fleetwood, L., Kaiser, R., Barros-Söderling, J., Bühler, R., Vallee, B. L., & Jörnvall, H. (1985) *Biochemistry 24*, 5303-5307.

Jörnvall, H., Hempel, J., Vallee, B. L., Bosron, W. F., & Li, T.-K. (1984) *Proc. Natl. Acad. Sci. U.S.A. 81*, 3024-3028.

Keung, W. M., Ditlow, C. C., & Vallee, B. L. (1985) *Anal. Biochem. 151*, 92-96.

Lowry, O. H., Rosebrough, N. J., Farr, A. L., & Randall, R. J. (1951) *J. Biol. Chem. 193*, 265-275.

Mårdh, G., Falchuk, K. H., Auld, D. S., & Vallee, B. L. (1986) *Proc. Natl. Acad. Sci. U.S.A. 83*, 2836-2840.

Smith, M., Hopkinson, D. A., & Harris, H. (1973) *Ann. Hum. Genet. 37*, 49-67.

Stamatoyannopoulos, G., Chen, S. H., & Fukui, M. (1975) *Am. J. Hum. Genet. 27*, 789-796.

Vallee, B. L., & Bazzone, T. J. (1983) in *Isozymes: Current Topics in Biological and Medical Research* (Scandalios, J. G., Rattazzi, M. C., & Whitt, G. S., Eds.) Vol. 8, pp 219-244, Alan R. Liss, New York.

von Wartburg, J.-P., Papenburg, J., & Aebi, H. (1965) *Can. J. Biochem. 43*, 889-898.

Wagner, F. W., Burger, A. R., & Vallee, B. L. (1983a) *Biochemistry 22*, 1857-1863.

Yin, S.-J., Bosron, W. F., Li, T.-K., Ohnishi, K., Okuda, K., Ishii, H., & Tsuchiya, M. (1984a) *Biochem. Genet. 22*, 169-180.

Yin, S.-J., Bosron, W. F., Magnes, L. J., & Li, T.-K. (1984b) *Biochemistry 23*, 5847-5853.

# Conformational Aspects and Rotational Dynamics of Synthetic Adrenocorticotropin-(1-24) and Glucagon in Reverse Micelles†

Jacques Gallay,*,‡,§ Michel Vincent,‡,§ Claude Nicot,§,∥ and Marcel Waks§,∥

*Laboratoire pour l'Utilisation du Rayonnement Electromagnétique du Centre National de la Recherche Scientifique, Bâtiment 209D, Université Paris Sud, 91405 Orsay Cedex, France, and Equipe de Recherche No. 64-01 and Unité Associée No. 586 du Centre National de la Recherche Scientifique, Université René Descartes, 75270 Paris Cedex 06, France*

*Received February 4, 1987; Revised Manuscript Received April 20, 1987*

ABSTRACT: The tryptophan (Trp) rotational dynamics and the secondary structure of the peptide hormones adrenocorticotropin-(1-24) [ACTH(1-24)]—the fully active N-terminal fragment of adrenocorticotropin-(1-39)—and glucagon were studied in aqueous solutions and in reverse micelles of sodium bis(2-ethylhexyl) sulfosuccinate (AOT)/water/isooctane, a system selected to mimick the membrane–water interface. In aqueous solutions, the total fluorescence intensity decays of their single Trp residue [Trp-9 and Trp-25 for ACTH(1-24) and glucagon, respectively] are multiexponential. This is also the case for ACTH(5-10), a fragment of the adrenocorticotropin "message" region. Time-resolved fluorescence anisotropy data evidence a high degree of rotational freedom of the single Trp residue. Transfer of these peptides from water to the aqueous core of reverse micelles induces severe restrictions of the Trp internal motion and of its local environment. The results indicate that the Trp-9 residue in ACTH(1-24) is maintained in the close neighborhood of the water–AOT molecular interface where the water molecules are strongly immobilized. By contrast, the Trp residues in ACTH(5-10) and glucagon are likely to be located closer to the center of the micellar aqueous core where the water molecules are in a more mobile state. Furthermore, the above location of Trp can be extended to the peptide chains themselves as evidenced by the overall correlation time values of the peptide-containing micelles. Nevertheless, in all peptides, the indole ring remains susceptible to oxidation by *N*-bromosuccinimide. Circular dichroism measurements evidence the induction in glucagon of $\alpha$-helices remaining unaffected by the micellar water content. Conversely, $\beta$-sheet structures are favored in ACTH(1-24) at low water-to-surfactant molar ratios ($w_0$) but are disrupted by subsequent additions of water. These results are discussed in terms of the possible role of the micellar interfaces in selecting the preferred peptide dynamical conformation(s).

The conformational adaptability of peptide hormones has been investigated in a variety of homogeneous solvents (Gratzer et al., 1968; Greff et al., 1976; Nabedryk-Viala et al., 1978; Toma et al., 1981, 1985). Further, the use of surfactant micelles and of lipid vesicles in water has provided a more accurate description of the peptide–hormone interactions with a membrane-like interface, since in these systems the anisotropic and amphipathic nature of biological membranes is preserved to a certain extent (Bornet & Edelhoch, 1971; Schneider & Edelhoch, 1972; Braun et al., 1983; Gremlich et al., 1983; Kaiser & Kézdy, 1983; Epand & Surewicz, 1984;

† This work was supported in part by grants from CNRS, INSERM, and Université Paris V.

* Address correspondence to this author at the Laboratoire pour l'Utilisation du Rayonnement Electromagnétique.

‡ Laboratoire pour l'Utilisation du Rayonnement Electromagnétique.

§ Equipe de Recherche No. 64-01.

∥ Unité Associée No. 586.

0006-2960/87/0426-5738$01.50/0 

Deber & Behnam, 1985). However in these model membranes experimental modifications of the physical state of the interfacial water, which can be a determining factor for the induction of the secondary structure of these peptides as well as for variations of their local internal motion, are not easily performed.

Reverse micelles are self-organized assemblies of surfactant, thermodynamically stable in organic solvents and in the presence of limited amounts of water. Such micelles are designated as reverse since their polar head groups concentrate in the aqueous interior of these spheroidal aggregates, while their hydrocarbon tails protrude into and are surrounded by the bulk apolar solvent. The key structural parameter of reverse micelles is the water-to-surfactant molar ratio $w_0$, which determines their size as well as the unusual physical–chemical properties of the entrapped water, markedly different from those of normal bulk water [for a review, see Luisi and Magid (1986)].

Depending upon its water content ($w_0$), the microscopic polarity and dielectric constant, the microviscosity, the water activity, the freezing point, and the proton transfer efficiency, as well as the hydrogen-bonding potential of the aqueous inner core, can be experimentally varied, providing thus a unique and versatile reaction field. Different, rapidly exchanging populations of water molecules were also found within reverse micelles, with less mobile molecules at the water–surfactant interface and more mobile molecules in the center of the micelle (the water pool).

Reverse micelles make the study of macromolecules in a restricted water environment possible; moreover, they are optically transparent. It seems obvious that the state of water, which can be modulated as a function of $w_0$ values, may influence the dynamics and the conformational states of the solubilized polypeptide chains. A peptide or a protein, in turn, will probably compete for hydration water with the charged polar head groups (Chatenay et al., 1985) and affect the state of the water and/or even perturb the dynamical equilibrium of the system (Chatenay et al., 1987).

In this study, we have incorporated the peptide hormones ACTH(1–24)[1] (the fully active N-terminal fragment of adrenocorticotropin), ACTH(5–10) [a part of the "message" region of the hormone (Schulster & Schwyzer, 1980)], and glucagon into the aqueous core of reverse micelles composed of sodium bis(2-ethylhexyl) sulfosuccinate (AOT) and water in isooctane. The variation of internal dynamics was investigated for each peptide at the level of their single Trp residue by steady-state and time-resolved fluorescence spectroscopy in aqueous solutions and in reverse micelles as a function of the water-to-surfactant molar ratio $w_0$. Circular dichroism measurements were carried out to characterize the peptide conformational changes occurring in reverse micelles. The results presented here suggest that, in addition to the specific amino acid sequence of each peptide, the physicochemical properties of the sequestered water and the interactions with the anionic head groups of the surfactant play a prominent role in the mechanism of the structural and dynamic adaptability of these peptides.

## Materials and Methods

*Chemicals.* Synthetic adrenocorticotropin-(1–24) [ACTH-(1–24)] (Chart Ia) was a generous gift of Drs. K. Scheibli and R. Andreatta from Ciba-Geigy (Basel, Switzerland); ACTH-(5–10) and glucagon (Chart Ib) were from Serva (Heidelberg, Germany); *N*-acetyl-L-Tryptophanamide (NATA) was purchased from Sigma Chemical Co. (St. Louis, MO); *p*-terphenyl and *N*-bromosuccinimide were from Koch-Light (Colnbrook Bucks, England); cyclohexane and isooctane (Uvasol grade) were from Merck (Darmstadt, FRG); glycerol (spectrophotometric grade) was from Eastman Kodak (Rochester, NY). Sodium bis(2-ethylhexyl) sulfosuccinate, a generous gift from the Cyanamid Co. (France), was purified according to Wong et al. (1976) and carefully dried in vacuo. The purity of each batch was checked according to the standards recommended by Luisi et al. (1984).

Chart I

a) ACTH(1-24):

```
 1                   6           9           12
Ser-Tyr-Ser-Met-Glu-His-Phe-Arg-Trp-Gly-Lys-Pro-
                                                24
Val-Gly-Lys-Lys-Arg-Arg-Pro-Val-Lys-Val-Tyr-Pro.
```

b) Glucagon:

```
 1                   6                       12
His-Ser-Gln-Gly-Thr-Phe-Thr-Ser-Asp-Tyr-Ser-Lys-
                                                24
Tyr-Leu-Asp-Ser-Arg-Arg-Ala-Gln-Asp-Phe-Val-Gln-
25
Trp-Leu-Met-Asn-Thr.
```

*Preparation of Reverse Micelles.* Reverse micelles of AOT and water in isooctane were prepared according to Nicot et al. (1985), at water-to-surfactant molar ratios ($w_0$ = $[H_2O]/[AOT]$) from 2.8 to 22.4 (i.e., 0.25–2% v/v at 50 mM AOT). Since micellar solutions are optically transparent, the concentration of solubilized peptides was determined spectrophotometrically by using molar extinction coefficients at 280 nm of $7.8 \times 10^3$ $M^{-1}\cdot cm^{-1}$ for ACTH(1–24), $5.5 \times 10^3$ $M^{-1}\cdot cm^{-1}$ for ACTH(5–10), and $8.3 \times 10^3$ $M^{-1}\cdot cm^{-1}$ for glucagon (Grätzer et al., 1968). Absorption measurements were carried out on a Cary 118 C spectrophotometer.

*Titration of Tryptophan.* The reaction of *N*-bromosuccinimide with tryptophan (Spande & Witkop, 1967) was carried out in micellar solutions as previously described by Nicot et al. (1985).

*Circular Dichroism.* CD measurements were performed on a Jobin et Yvon Mark V spectropolarimeter. The wavelength range scanned was 200–350 nm. The spectra of peptide-containing micelles were corrected by substracting blank runs of peptide-free micellar solutions performed at appropriate $w_0$ values. The reported spectra are the average of several scans. Ellipticity values ($\theta$) are expressed on a mean residue basis in units of $deg\cdot cm^2\cdot dmol^{-1}$. No correction was made since the solutions are devoid of scattering.

*Fluorescence Measurements.* Corrected fluorescence emission spectra (4-nm bandwidth) were recorded on a SLM 8000 spectrofluorometer coupled to a Hewlett-Packard 9815 A minicomputer. "Magic angle" configuration [excitation polarizer in the vertical position and emission polarizer at 55° from the vertical (Spencer & Weber, 1970)] was used. Excitation wavelength was 295 nm (2-nm bandwidth). The

[1] Abbreviations: ACTH(1–24), synthetic adrenocorticotropin-(1–24); ACTH(5–10), synthetic adrenocorticotropin-(5–10); AOT, sodium bis-(2-ethylhexyl) sulfosuccinate; CD, circular dichroism; $^1H$ NMR, proton nuclear magnetic resonance; NATA, *N*-acetyl-L-tryptophanamide.

temperature of the sample, in a 1 × 1 cm quartz cell, was regulated with a circulating water thermostat (Hüber HS 40).

Steady-state anisotropy measurements were performed on the same apparatus in the T-format configuration. The emission light was collected through a 1 M $CuSO_4$ cut-off filter (1-cm optical path in a quartz cell). For intrinsic anisotropy spectra, 97–100% (v/v) glycerol solutions of ACTH(1–24) ($1.8 \times 10^{-5}$ M), ACTH(5–10) ($7 \times 10^{-5}$ M), and NATA ($2.7 \times 10^{-5}$ M) were prepared, and the measurements were performed at −38 °C. The temperature was monitored with a thermistor probe coupled to a digital thermometer. The background fluorescence from glycerol was substracted. In these measurements, a 1-nm excitation bandwidth was used.

Time-resolved fluorescence anisotropy decay measurements were performed by the time-correlated single-photon method (Yguerabide, 1972; Wahl, 1975) on the instrument at LURE (Laboratoire pour l'Utilisation du Rayonnement Electromagnétique) (Jameson & Alpert, 1979; Brochon, 1980), with as the light source the synchrotron radiation generated by the electron storage ring of ACO (Anneau de Collision d'Orsay), working at a frequency of 13.6 MHz in a single-bunch mode. The excitation pulse displayed FWHM of 1.4 ns. Briefly, the single photon counting instrument consisted of a SLM holographic double monochromator to select the excitation wavelength (295 nm, bandwidth 2 nm). Vertically polarized light was obtained through a Glan-Thomson polarizer. The emission fluorescence was collected through a 1 M $CuSO_4$ cut-off filter (in a quartz cell of 1-cm optical path). $I_{vv}(t)$ and $I_{vh}(t)$ curves were collected alternatively each 20 or 30 s through a polaroid film. Counting electronics were from Ortec. The data were stored in a 512-channel memory of a MCA Nuclear Data ND 660 microcomputer. Experiments were stopped when 15 000–20 000 counts were obtained in the difference curves. The apparatus response function was obtained with the short lifetime standard *p*-terphenyl ($\tau = 0.95$ ns in cyclohexane; Berlman, 1971), according to Wahl et al. (1974).

Data were analyzed by a nonlinear least-squares procedure (Grinvald & Steinberg, 1974; Wahl, 1979; Mérola & Brochon, 1986) as a sum of exponentials: $r(t) = \sum_i \beta_i \exp(-t/\phi_i)$. The fitting criteria were the minimum $\chi^2$ values and the pattern of the deviation functions. Typically, a biexponential model was sufficient to minimize the $\chi^2$ in most cases; a triple exponential did not improve the accuracy of the fit.

Total fluorescence intensity decay measurements and analysis were performed on a time-correlated single photon counting instrument, described in previous publications (Vincent et al., 1985) and equipped with the nanosecond thyratron-gated flash lamp from Edinburgh Instruments (Birch & Imhof, 1981). Typically, the lamp was run in ≃0.9 atm of nitrogen with an electrode gap of 0.6 mm. Repetition rate was 30 kHz, with a power supply of 7 kV. The excitation wavelength was selected at 296 nm (5-nm bandwidth) with a grating monochromator blazed at 300 nm (Applied Photophysics). When the excited-state lifetimes were measured as a function of the emission wavelength, the fluorescence was collected through a similar monochromator (20-nm bandwidth). Magic angle configuration (excitation polarizer at 35° from the vertical, no polarizer at the emission side) was set to allow minimization of polarization bias (Spencer & Weber, 1970). For measurements of the decay over the full spectrum, a 1 M $CuSO_4$ cut-off filter was used (1-cm optical path).

## Results

*Steady-State Fluorescence Spectra.* The fluorescence emission spectra of ACTH(1–24), ACTH(5–10), and glucagon were recorded in buffer and in micellar solutions of AOT/water/isooctane, at various water-to-surfactant molar ratios ($w_0$). In aqueous solutions, the emission maxima are 348 nm for ACTH(1–24) and 352 nm for both ACTH(5–10) and glucagon. Under similar conditions, the maximum emission of the model compound *N*-acetyl-L-tryptophanamide (NATA) is 357 nm (Nicot et al., 1985). Upon incorporation of the peptides into reverse micelles at high $w_0$ values (>8), a blue shift of the emission maximum is observed (Figure 1). ACTH(1–24) displays the largest effect in the $w_0$ range 22.4–8. Glucagon and ACTH(5–10) behave as NATA. At low $w_0$ values (<8), a further blue shift is observed for the three peptides and for NATA as well. It should be remarked that, for very low $w_0$ values (<2.8), ACTH(1–24) and glucagon are sparingly soluble in reverse micelles, their solubility increasing with the water content of the system (data not shown).

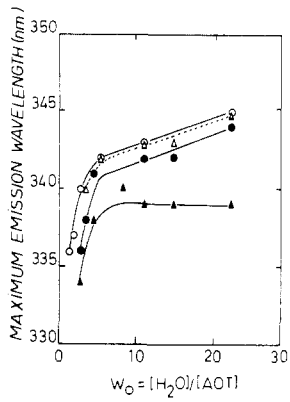


FIGURE 1: Variation of the maximum emission wavelength of ACTH(1–24) (▲), glucagon (●), ACTH(5–10) (△), and NATA (○) as a function of the water-to-surfactant molar ratio ($w_0$) in reverse micelles. Experimental conditions are described under Materials and Methods.

*Total Fluorescence Intensity Decay Measurements in Aqueous Solutions.* Whatever the peptide studied, the total fluorescence intensity decay of their single Trp residue does not follow a simple exponential law as illustrated in Figure 2A (upper panel). According to $\chi^2$ minimization and deviation function criteria, a double-exponential model strickingly improves the fit of the experimental data (Figure 2A, lower panel). The total intensity decay parameters for the double-exponential model are reported in Table I. For ACTH(1–24) and glucagon, the results show slightly shorter lifetime values as compared to those reported by Ross et al. (1981) but are in good agreement with the data published by Cockle and Szabo (1981) and Tran et al. (1982). To the best of our knowledge, the total fluorescence intensity decay of ACTH-(5–10) has never been reported. This peptide exhibits a higher mean excited state lifetime value than ACTH(1–24), mainly arising from the higher contribution of the long-lifetime component. The short- and long-lifetime values are the same in both peptides. In agreement with Ross et al. (1981), the total emission kinetic parameters of ACTH(1–24) are independent of the emission wavelength, and the mean excited state lifetime remains constant through the emission spectrum (Figure 3A). A similar trend was observed for ACTH(5–10) (data not shown). For the model compound NATA, a monoexponential decay law is sufficient to minimize the $\chi^2$ value. The excited-state lifetime value is 2.96 ± 0.05 ns ($\chi^2 = 1.1$), in agreement with published data (Privat et al., 1979; Ross et al., 1981).

*Total Fluorescence Intensity Decay Measurements in Reverse Micelles.* As in aqueous solutions, the total fluorescence intensity decay of the peptides is not monoexponential. A

Table I: Trp Fluorescence Intensity Decay Parameters in Peptide Hormones in 0.1 M Phosphate Buffer, pH 7.6, and in Reverse Micelles at Various $w_0$ Values[a]

| | $w_0$ | $\tau_1$ (ns) | $\tau_2$ (ns) | $\alpha_1$ | $\alpha_2$ | $\langle\tau\rangle$ (ns)[b] | $\chi^2$ |
|---|---|---|---|---|---|---|---|
| ACTH(1-24) | 2.8 | 4.30 | 1.31 | 0.44 | 0.56 | 3.46 | 1.5 |
| | 5.6 | 4.06 | 1.42 | 0.32 | 0.68 | 2.93 | 1.4 |
| | 8.4 | 3.92 | 1.37 | 0.26 | 0.74 | 2.65 | 1.3 |
| | 15.0 | 3.60 | 1.26 | 0.28 | 0.72 | 2.48 | 1.3 |
| | 22.4 | 3.66 | 1.25 | 0.26 | 0.74 | 2.47 | 1.5 |
| | buffer | 3.45 | 0.93 | 0.50 | 0.50 | 2.92 | 1.9 |
| ACTH(5-10) | 2.8 | 3.80 | 1.04 | 0.36 | 0.64 | 2.89 | 1.7 |
| | 3.5 | 3.75 | 1.07 | 0.35 | 0.65 | 2.81 | 1.5 |
| | 5.6 | 3.70 | 1.17 | 0.31 | 0.69 | 2.64 | 1.8 |
| | 11.2 | 3.32 | 1.04 | 0.30 | 0.70 | 2.35 | 1.8 |
| | 15.0 | 3.28 | 0.97 | 0.30 | 0.70 | 2.32 | 1.6 |
| | 22.4 | 3.14 | 1.02 | 0.31 | 0.69 | 2.25 | 1.4 |
| | buffer | 3.47 | 1.11 | 0.61 | 0.39 | 3.08 | 0.9 |
| glucagon | 3.5 | 4.08 | 1.14 | 0.27 | 0.73 | 2.82 | 1.5 |
| | 5.6 | 3.91 | 1.14 | 0.19 | 0.81 | 2.37 | 1.7 |
| | 11.2 | 3.75 | 0.95 | 0.16 | 0.84 | 2.13 | 2.1 |
| | 22.4 | 3.74 | 0.84 | 0.16 | 0.84 | 2.18 | 3.2 |
| | buffer | 3.74 | 1.10 | 0.51 | 0.49 | 3.15 | 1.7 |
| NATA | 2.0 | 3.41 | 1.13 | 0.44 | 0.56 | 2.73 | 1.9 |
| | 22.4 | 3.50 | 1.51 | 0.10 | 0.90 | 1.91 | 1.6 |
| | buffer | 2.96 | | | | | 1.1 |

[a] Excitation wavelength: 295 nm (5-nm bandwidth). Emission: 1 M $CuSO_4$ filter (1-cm optical path). Magic angle configuration: excitation polarizer vertical-emission polarizer at 55° from the vertical (Spencer & Weber, 1970). Temperature: 20 °C. $OD_{295nm} \simeq 0.1$. Biexponential model: $i(t) = \alpha_1 \exp(-t/\tau_1) + \alpha_2 \exp(-t/\tau_2)$. [b] Calculated from $\langle\tau\rangle = \sum_i a_i\tau_1^2/\sum a_i\tau_i$ (Inokuti & Hirayama, 1965).

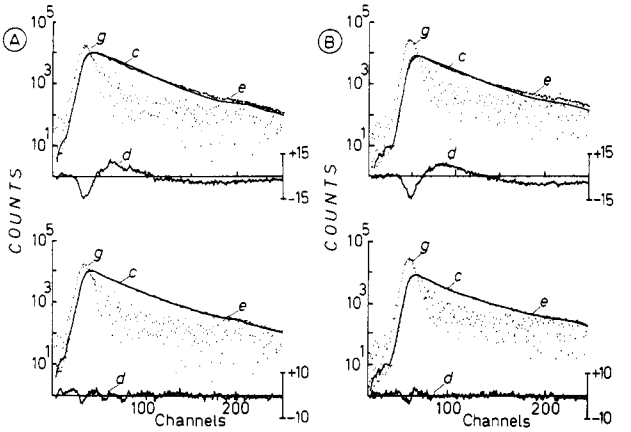


FIGURE 2: (A) Total fluorescence intensity decay of ACTH(1-24) in 0.1 M phosphate buffer, pH 7.6: (g) apparatus response function calculated according to Wahl et al. (1974); (c) (solid line) lamp convolved curve; (e) (dotted line) experimental decay curve; (d) deviation function. Time calibration: 0.099 ns/channel. (Upper panel) Monoexponential model ($\tau$ = 2.81 ns, $\chi^2$ = 20.19). (Lower panel) Biexponential model ($\tau_1$ = 0.93 ns, $\tau_2$ = 3.45 ns, $a_1$ = 0.496, $a_2$ = 0.504, $\chi^2$ = 1.96). Mean excited state lifetime $\langle\tau\rangle$ = 2.92 ns, calculated from $\langle\tau\rangle = \sum_i a_i\tau_i^2/\sum_i a_i\tau_i$ (Inokuti & Hirayama, 1965). (B) Total fluorescence intensity decay of ACTH(1-24) in reverse micelles ($w_0$ = 2.8). Same symbols as in (A). (Upper panel) Monoexponential model ($\tau$ = 3.09 ns, $\chi^2$ = 26.58). (Lower panel) Biexponential model ($\tau_1$ = 1.21 ns, $\tau_2$ = 4.25 ns, $a_1$ = 0.60, $a_2$ = 0.40, $\chi^2$ = 1.52), $\langle\tau\rangle$ = 3.34 ns. Other experimental conditions as in Table I and under Materials and Methods.

biexponential model, providing a correct fit of the data, was used in all experiments, including total intensity decay measurements as a function of the emission wavelength. This is illustrated for ACTH(1-24) in Figure 2B. Upon incorporation of the hormonal peptides into reverse micelles, two effects are observed. First, the mean excited state lifetime ($\langle\tau\rangle$), measured over the full emission spectrum, is decreased in reverse micelles of high water content as compared to water solutions (Table I). Second, its value becomes higher than that in aqueous solutions, as the micellar water content is decreased. Studies of the emission wavelength dependence of the total intensity decay reveal that, in contrast to its behavior in aqueous solutions, the mean excited state lifetime of ACTH-

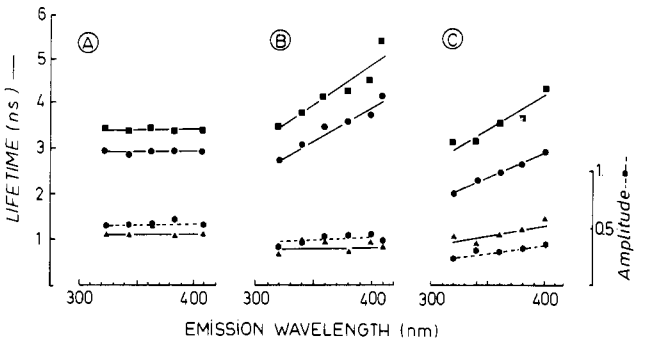


FIGURE 3: Emission wavelength dependence of the total fluorescence intensity decay parameters of ACTH(1-24). The decay curves were analyzed as in Figure 2. (●) Mean excited state lifetime $\langle\tau\rangle$; (▲) $\tau_1$; (■) $\tau_2$; (●) $a_2$. (A) ACTH(1-24) in buffer; (B) ACTH(1-24) in reverse micelles at $w_0$ = 3.5; (C) ACTH(1-24) in reverse micelles at $w_0$ = 22.4. Experimental conditions as under Materials and Methods.

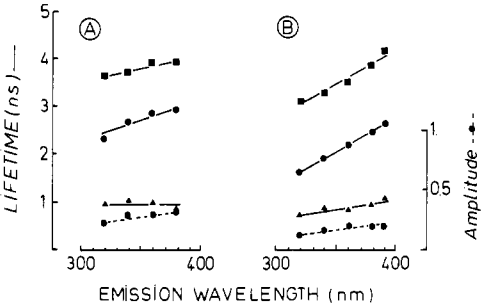


FIGURE 4: Emission wavelength dependence of the total fluorescence intensity decay parameters of glucagon in reverse micelles. The decay curves were analyzed as in Figure 2. (●) Mean excited state lifetime $\langle\tau\rangle$; (▲) $\tau_1$; (■) $\tau_2$; (●) $a_2$. Water-to-surfactant molar ratios: (A) $w_0$ = 3.5; (B) $w_0$ = 22.4.

(1-24) is progressively increased in the red edge region of the emission spectrum (Figure 3B,C). Whatever the water content of the micelles, a similar variation of the mean excited state lifetime with the emission wavelength is observed [$\Delta\langle\tau\rangle = \langle\tau\rangle_{400nm} - \langle\tau\rangle_{320nm}$ = 0.98 and 0.80 ns at $w_0$ = 3.6 and 22.4, respectively]. At low $w_0$ values, this enhancement is almost exclusively the result of an increase of the long time compo-

Table II: Trp Steady-State Fluorescence Anisotropy Values and Time-Resolved Fluorescence Anisotropy Decay Parameters of ACTH(1–24), ACTH(5–10), Glucagon, and NATA in 0.1 M Phosphate Buffer, pH 7.6, 20 °C[a]

| | $r$ | $r_0$[b] | $r_{0\,eff}$[c] | $\phi_1$ (ns) | $\phi_2$ (ns) | $\beta_1$ | $\beta_2$ | $\chi^2$ |
|---|---|---|---|---|---|---|---|---|
| ACTH(1–24) | 0.35 | 0.199 | 0.194 ± 0.056 | 0.15 ± 0.08 | 1.56 ± 0.12 | 0.107 ± 0.047 | 0.087 ± 0.011 | 1.1 |
| ACTH(5–10) | 0.012 | 0.188 | 0.238 ± 0.020 | 0.07 ± 0.02 | 0.48 ± 0.10 | 0.172 ± 0.008 | 0.066 ± 0.016 | 1.1 |
| glucagon | 0.040 | | 0.192 ± 0.033 | 0.16 ± 0.01 | 1.42 ± 0.04 | 0.106 ± 0.016 | 0.086 ± 0.016 | 1.0 |
| NATA | | 0.181 | 0.215 ± 0.039 | 0.03 ± 0.01 | | 0.215 ± 0.039 | | 1.4 |

[a] Excitation wavelength: 295 nm (2-nm bandwidth). Emission: 1 M $CuSO_4$ (1-cm optical path). Biexponential model: $r(t) = \beta_1 \exp(-t/\phi_1) + \beta_2 \exp(-t/\phi_2)$. [b] Measured in glycerol at −38 °C. [c] $r_{0\,eff} = \beta_1 + \beta_2$.

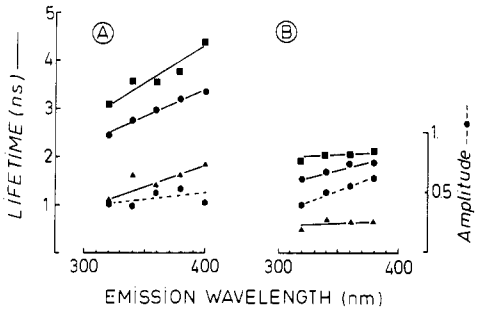


FIGURE 5: Emission wavelength dependence of the total fluorescence intensity decay parameters of NATA in reverse micelles. The decay curves were analyzed as in Figure 2. (●) Mean excited state lifetime $\langle\tau\rangle$; (▲) $\tau_1$; (■) $\tau_2$; (●) $a_2$. Water-to-surfactant molar ratios: (A) $w_0 = 2.0$; (B) $w_0 = 22.4$.

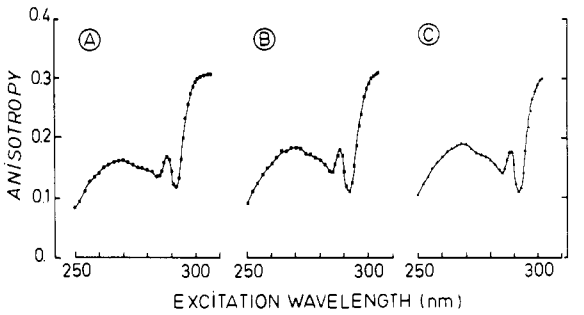


FIGURE 6: Intrinsic fluorescence anisotropy spectrum in vitrified medium (glycerol, −38 °C) of (A) ACTH(1–24) ($1.8 \times 10^{-5}$ M), (b) ACTH(5–10) ($7.1 \times 10^{-5}$ M), and (c) NATA ($2.7 \times 10^{-5}$ M). Excitation bandwidth: 1 nm.

nent. At high $w_0$ values, the short time component is also increased, but only to a slight extent (Figure 3B,C). For glucagon, similar features are observed (Figure 4). However, in contrast to ACTH(1–24), the wavelength dependence of the mean excited state lifetime is less important at low (3.6) than at high (22.4) $w_0$ [$\Delta\langle\tau\rangle = \langle\tau\rangle_{400nm} - \langle\tau\rangle_{320nm} = 0.80$ and 1.12 ns for each $w_0$ value, respectively].

By contrast to water solution, the total fluorescence intensity decay of NATA is not monoexponential in reverse micelles. The insertion of this compound into the micellar system results in two effects with respect to the mean excited state lifetime variations, as observed for the peptides. At high $w_0$, this parameter is decreased whereas at low $w_0$ values it is enhanced to reach values close to that in water solutions. Decay measurements through the emission spectrum evidence an increase of the mean excited state lifetime with the emission wavelength. At low water content, both lifetime components are increased as well as the amplitude of the long one. At high $w_0$, only the relative amplitudes are changed as a function of the emission wavelength, the lifetime component remaining invariant through the emission spectrum (Figure 5).

*Fluorescence Anisotropy Studies in Aqueous Solutions.* The fluorescence anisotropy excitation spectrum of each polypeptide in vitrified glycerol exhibits the classical pattern already described in the literature for tryptophan and indole (Valeur & Weber, 1977), with some changes in the region where tyrosine residues contribute to the fluorescence emission (Figure 6A,B). The spectrum of NATA was measured as a control. In aqueous solutions, the steady-state fluorescence anisotropy values of each peptide are low, indicating a high degree of rotational freedom (Table II). Time-resolved fluorescence anisotropy decay data were analyzed with mono- and biexponential models. For all peptides, the second model provides the best fit to the data, as exemplified for ACTH(1–24) in Figure 7A. A very short correlation time of about 0.1 ns and a second one longer by 1 order of magnitude are measured. The values of the anisotropy at zero time of the decay are close to the intrinsic anisotropy values measured in vitrified glycerol, at the same excitation wavelength of 295 nm (Table II). The short time component can be ascribed to the internal motion of the Trp residue within the peptide matrix

Table III: Average Restricted Rotation Angle of the Trp Residue in ACTH(1–24), ACTH(5–10), and Glucagon in 0.1 M Phosphate Buffer, pH 7.6

| peptide | $\theta_1$ (deg)[a] | $\theta_2$ (deg)[b] |
|---|---|---|
| ACTH(1–24) | 41 | 28 |
| glucagon | 41 | 29 |
| ACTH(5–10) | 46 | 31 |

[a] Calculated from $\beta_2/r_0 = [(1/2 \cos\theta_1)(1 + \cos\theta_1)]^2$ (Kinosita et al., 1977). [b] Calculated from $\beta_2/r_0 = [(3\cos^2\theta_2 - 1)/2]^2$ (Wallach, 1967; Lipari & Szabo, 1980).

(Gottlieb & Wahl, 1963; Lakowicz et al., 1983), and an average restricted angle of rotation can be calculated (Wallach, 1967; Kinosita et al., 1977; Lipari & Szabo, 1980) (Table III). For glucagon, the results are in agreement with those of Tran et al. (1982), although performed at different pH values. For ACTH(1–24) and ACTH(5–10), the fluorescence anisotropy decays have not been reported to the best of our knowledge under the conditions of the present work: in absence of sucrose and at ambient temperature. The long correlation time corresponding to the overall tumbling of both peptides exhibits small values in agreement with their molecular weights (Table II).

*Fluorescence Anisotropy Studies in Reverse Micelles.* The incorporation of the peptides and NATA into reverse micelles increases the steady-state fluorescence anisotropy value of the fluorophore to a large extent. As in aqueous solutions, the fluorescence anisotropy decays of the peptides can be fitted by biexponential functions (Figure 7B). Both correlation times are increased by 1 order of magnitude as compared to aqueous solutions. The short correlation time remains unsensitive to variation of $w_0$ (Table IV). The average restricted angle of rotation is more limited for all peptides as compared to aqueous solutions (Table III and Figure 8). For ACTH(1–24), this angle remains independent of the water micellar content, whereas for the uncharged peptides it increases with the amount of water present (Figure 8). The anisotropy at zero time is lower than the intrinsic anisotropy value measured in vitrified glycerol, more especially for ACTH(1–24) (Figure 7B). The variation of the long correlation time as a function of the water micellar content is illustrated on Figure 9. The variation of the theoretical micellar correlation time as cal-

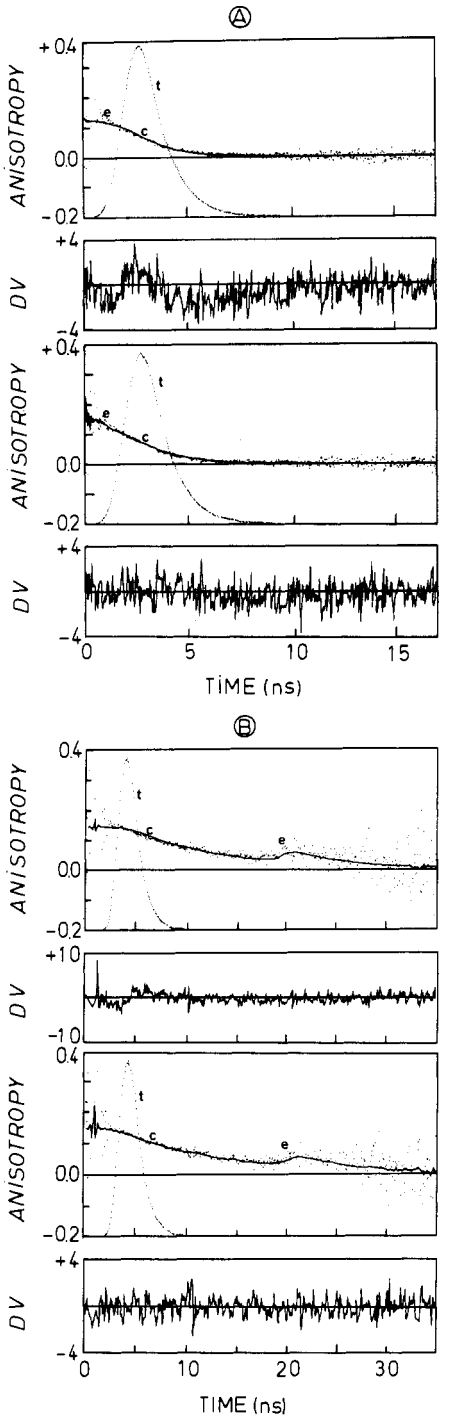


FIGURE 7: Fluorescence anisotropy decay of Trp-9 in ACTH(1-24): (t) *p*-terphenyl total intensity decay; (c) (—) calculated curve; (e) (···) experimental curve; (DV) deviation function. (A) ACTH(1-24) in buffer. Time calibration: 0.047 ns/channel. (Upper panel) Monoexponential model ($\phi$ = 1.02 ns; $r_{0\,eff}$ = 0.137, $\chi^2$ = 2.16); (lower panel) biexponential model ($\phi_1$ = 0.10 ± 0.04 ns; $\phi_2$ = 1.59 ± 0.06 ns; $\beta_1$ = 0.106 ● 0.019; $\beta_2$ = 0.081 ± 0.004; $r_{0\,eff}$ = 0.187; $\chi^2$ = 1.07). (B) ACTH(1-24) in reverse micelles, $w_0$ = 5.6. Time calibration: 0.090 ns/channel. (Upper panel) Monoexponential model ($\phi$ = 9.24 ± 0.14; $r_{0\,eff}$ = 0.142 ± 0.001; $\chi^2$ = 1.37); (lower panel) biexponential model ($\phi_1$ = 0.58 ± 0.16 ns; $\phi_2$ = 11.30 ± 0.38 ns; $\beta_1$ = 0.030 ± 0.003; $\beta_2$ = 0.128 ± 0.002 ns; $r_{0\,eff}$ = 0.158; $\chi^2$ = 1.01).

culated from the Stokes-Einstein relation ($\phi = \eta V/RT$), assuming the micelle to be a perfect rotating sphere, is also represented. The micelle radii are in the range from 22 to 50 Å between $w_0$ values of 2.8 and 22.4 (Chatenay et al., 1985). Between $w_0$ values from 2 to 6, the increase of the measured correlation time parallels that of the calculated one. Above these $w_0$ values, the two curves diverge, the measured correlation time values increasing less than the calculated ones. This is especially the case for glucagon- and ACTH(5-10)-containing micelles (Figure 9).

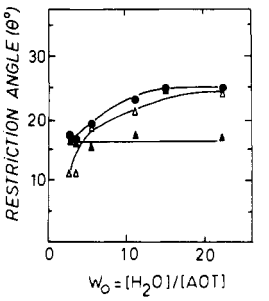


FIGURE 8: Variation of the restriction angle ($\theta$) of the Trp residue rotation in the peptides as a function of $w_0$. $\theta$ was calculated from the expression: $\beta_2/r_0 = [(3\cos^2\theta - 1)/2]^2$ (Wallach, 1967; Lipari & Szabo, 1980). (▲) ACTH(1-24); (●) glucagon; (△) ACTH(5-10).

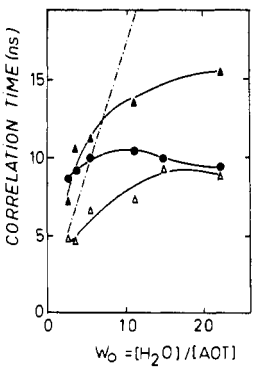


FIGURE 9: Variation of the long correlation time of the Trp fluorescence anisotropy decay in the peptide inserted into reverse micelles as a function of $w_0$. (▲) ACTH(1-24); (●) glucagon; (△) ACTH(5-10). (-·-) Variation of the rotational correlation time of the micelles calculated from the Stokes-Einstein relation: ($\phi = \eta V/kT$)$\eta_{20°C}$ = 0.54 cP is the viscosity of isooctane. The micelle radii were taken from Chatenay et al. (1985).

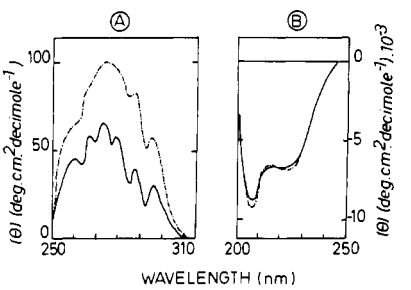


FIGURE 10: Near- (A) and far- (B) ultraviolet CD spectra of glucagon in micellar solutions of AOT (25 mM)/isooctane/water, at $w_0$ values of 3.5 (—) and 22.4 (-·-). The curves are an average of several measurements.

In the case of NATA, a strong slowing down of the rotational motion is also observed in the micelles as compared to water (Table IV). The data, analyzed by a biexponential model, show that both correlation times are only slightly sensitive to the micellar water content. At low $w_0$ values, the long correlation time dominates the decay whereas the converse is true at high $w_0$ values.

*Circular Dichroism.* All the peptides studied display in the near-ultraviolet dichroic bands characteristic of aromatic chromophores and are unaffected by the AOT concentration in the 18-150 mM range. These bands vary in sign according to the specific peptide and in intensity as the water content of the micelles. Figure 10A shows a typical CD spectrum of glucagon in the 250-350-nm range. In 50 mM AOT, for a $w_0$ value of 3.5, it displays a set of well-resolved positive bands at about 260, 268, 273, 279, 288, and 297 nm, unambiguously

Table IV: Fluorescence Anisotropy Decay of Peptides and NATA in Reverse Micelles as a Function of $w_0$[a]

| | $w_0$ | $r$ | $r_{0\,eff}$[b] | $\phi_1$ (ns) | $\phi_2$ (ns) | $\beta_1$ | $\beta_2$ | $\chi^2$ |
|---|---|---|---|---|---|---|---|---|
| ACTH(1–24) | 3.7 | 0.120 | 0.189 | 1.2 ± 0.4 | 10.6 ± 0.6 | 0.024 ± 0.004 | 0.132 ± 0.005 | 1.1 |
| | 5.6 | 0.123 | 0.160 | 0.5 ± 0.2 | 11.2 ± 0.4 | 0.030 ± 0.003 | 0.130 ± 0.003 | 1.0 |
| | 11.2 | 0.128 | 0.149 | 1.4 ± 0.4 | 13.5 ± 0.1 | 0.034 ± 0.005 | 0.115 ± 0.005 | 1.1 |
| | 22.4 | 0.128 | 0.151 | 1.3 ± 0.3 | 15.5 ± 0.2 | 0.036 ± 0.004 | 0.115 ± 0.005 | 1.1 |
| glucagon | 3.5 | 0.119 | 0.189 | 0.4 ± 0.1 | 9.1 ± 0.3 | 0.036 ± 0.006 | 0.153 ± 0.003 | 1.0 |
| | 5.6 | 0.128 | 0.183 | 0.5 ± 0.1 | 10.1 ± 0.5 | 0.044 ± 0.004 | 0.139 ± 0.003 | 1.2 |
| | 11.2 | 0.128 | 0.180 | 0.5 ± 0.1 | 10.5 ± 0.7 | 0.064 ± 0.005 | 0.116 ± 0.004 | 0.9 |
| | 22.4 | 0.119 | 0.196 | 0.5 ± 0.1 | 9.5 ± 0.6 | 0.090 ± 0.004 | 0.106 ± 0.003 | 1.0 |
| ACTH(5–10) | 5.6 | 0.112 | 0.183 | 0.9 ± 0.2 | 6.6 ± 0.3 | 0.047 ± 0.005 | 0.136 ± 0.006 | 1.1 |
| | 11.2 | 0.110 | 0.183 | 0.8 ± 0.1 | 7.3 ± 0.4 | 0.060 ± 0.004 | 0.123 ± 0.005 | 1.1 |
| | 22.4 | 0.109 | 0.183 | 0.9 ± 0.1 | 8.9 ± 0.7 | 0.076 ± 0.004 | 0.107 ± 0.007 | 1.1 |
| NATA | 1.4 | 0.104 | 0.218 | 1.4 ± 0.2 | 4.5 ± 0.5 | 0.110 ± 0.019 | 0.108 ± 0.020 | 1.3 |
| | 2.8 | 0.102 | 0.199 | 1.1 ± 0.2 | 4.1 ± 0.2 | 0.052 ± 0.010 | 0.147 ± 0.011 | 1.1 |
| | 5.6 | 0.090 | 0.208 | 0.9 ± 0.1 | 3.8 ± 0.5 | 0.095 ± 0.015 | 0.113 ± 0.020 | 1.3 |
| | 15.0 | 0.070 | 0.159 | 0.6 ± 0.1 | 3.8 ± 0.6 | 0.105 ± 0.007 | 0.054 ± 0.009 | 1.2 |
| | 22.4 | 0.068 | 0.174 | 0.4 ± 0.1 | 3.7 ± 0.4 | 0.111 ± 0.004 | 0.063 ± 0.005 | 1.1 |

[a] Biexponential model: $r(t) = \beta_1 \exp(-t/\phi_1) + \beta_2 \exp(-t/\phi_2)$. Excitation wavelength: 295 nm (2-nm bandwidth). Emission: 1 M $CuSO_4$ cutoff filter. Temperature: 20 °C. [b] $r_{0\,eff} = \beta_1 + \beta_2$.

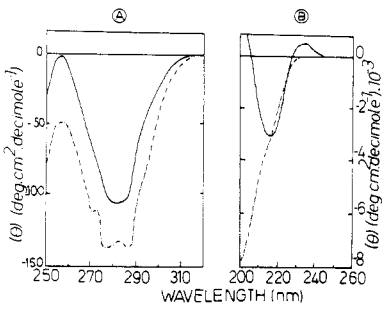


FIGURE 11: Near- (A) and far- (B) ultraviolet CD spectra of ACTH(1–24) in micellar solutions at 25 mM AOT and at $w_0$ values of 3.5 (—) and 22.4 (-·-).

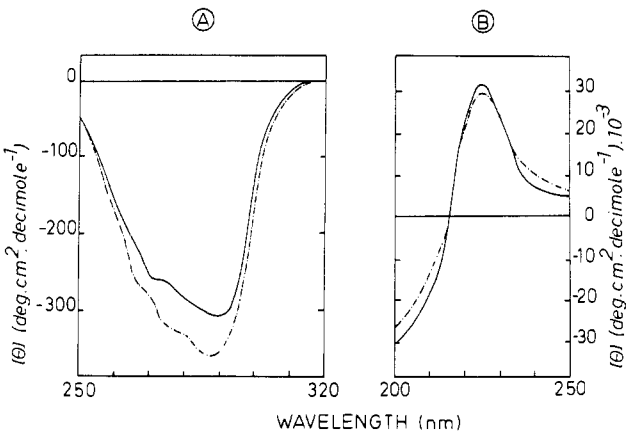


FIGURE 12: Near- (A) and far- (B) ultraviolet CD spectra of ACTH(5–10) in micellar solutions at 25 mM AOT and at $w_0$ values of 3.5 (—) and 22.4 (-·-).

related to the $L_b$ transition of Trp. At a high micellar water content ($w_0$ = 22.4), the resolution of these bands is partially lost. The maximum of the resulting broad band is centered at 279 nm, and the two minor bands at 260 and 268 nm remain at unchanged wavelengths. At the same time, the maximum intensity increases from $[\theta]$ = 65 to $[\theta]$ = 100 deg·cm²·dmol⁻¹ for $w_0$ = 3.5 and 22.4, respectively. The near-ultraviolet spectra of ACTH(1–24) and ACTH(5–10) both display broad negative bands between 250 and 320 nm. Their respective intensities are also enhanced with increased water-to-surfactant molar ratios (Figures 11A and 12A).

The CD spectra of glucagon, inserted in reverse micelles, exhibit in the far-ultraviolet (200–250 nm) a profile characteristic of an $\alpha$-helix, with minima at 208 and 222 nm and molar ellipticities of −9200 and −7500 deg·cm²·dmol⁻¹, respectively (Figure 10B). These values are nearly unaffected by the amount of water present in the $w_0$ range from 3.5 to 22.4.

By contrast, the conformation of ACTH(1–24) dramatically depends of the amount of water present in the micellar system (Figure 11B). At $w_0$ = 22.4, the peptide is largely unfolded, as evidenced by the negative extremum near 200 nm. A weak inflexion in the spectrum around 216 nm suggests however the possibility of some $\beta$-structure. At low water content ($w_0$ = 3.5), the negative band is shifted from 200 to 216 nm with a crossover at 205 nm and an intensity reduced by more than a half, from −7800 to −3100 deg·cm²·dmol⁻¹. These spectral features are consistent with the presence of a significant amount of $\beta$-pleated sheet. Figure 11B also shows the appearance at 235 nm of an additional positive band probably attributable to the $L_a$ transition of the sole Trp-9. This transition normally occurs at 220–235 nm, but in this case, it is overlapped by the negative dichroic band of the peptide-bond chromophore. The overlap causes this effective positive maximum to be shifted to the red, appearing at ≃235 nm. The negative wobble at 222 nm may also be due to the aromatic side chain.

The short ACTH(5–10) peptide displays in the same wavelength range a positive dichroic band near 225 nm of constant intensity at all the $w_0$ values studied. It can be mainly considered as the contribution of the Trp $L_a$ transition, with some phenylalanine contribution as well (Figure 12). In this work, we have not attempted a precise estimation of relative proportions of different forms of periodic secondary structure, since such estimation from CD spectra for small peptides is generally of poor accuracy (Woody, 1985).

*Reactivity of Trp Residues with N-Bromosuccinimide.* The Trp residues of the studied peptides were titrated with *N*-bromosuccinimide, a water-soluble reagent, at $w_0$ = 3.5 and 11.2, in micellar solutions. For all the peptides an average value of 0.74 ± 0.08 equiv/mol was titrated, and 4.0 equiv of *N*-bromosuccinimide was consumed, indicating the specificity of the reaction (Spande & Witkop, 1967).

## Discussion

Conformational studies have suggested that short, biologically active peptides devoid of intrachain cross-links exist in dilute solutions as an ensemble of conformers of approximately equal energy [for reviews, see Blundell and Wood (1982) and Schiller (1985)].

*Trp Environment and Dynamics in Aqueous Solutions of Peptides.* Multiexponential decays of the total fluorescence intensity are observed for the peptides in solution as already

reported for ACTH(1–24) and glucagon (Grinvald & Steinberg, 1976; Cockle & Szabo, 1981; Ross et al., 1981; Tran et al., 1982). This is also the case for ACTH(5–10). In the present study, the comparison between the fluorescence emission kinetic characteristics of ACTH(5–10) and ACTH-(1–24) suggests that the Trp-9 environment is very similar in both peptides despite the removal of a large part of the peptide chain. Hence, it appears that the interactions of the Trp-9 with the nearest-neighbor amino acids exert the main effect on its fluorescence emission kinetics but leave unaffected its excited-state energy level. Most likely the guanidinium quenching group of Arg-8 is of primary importance in that respect, as suggested by Ross et al. (1981). By contrast, in glucagon the existence of conformational substates in rapid exchange seems to be mainly responsible for the multiexponential total intensity decay of Trp-25 (Cockle & Szabo, 1981). Indeed, in glucagon-(23–26), which does not exhibit any organized structure in solution (Deranleau et al., 1978), the fluorescence intensity decay characteristics are quite different from those of uncleaved glucagon (Ross et al., 1981; Cockle & Szabo, 1981).

Fluorescence anisotropy decay measurements point to the existence of rotational hindrances to the Trp motion within the peptide matrix that can be the result of local structures. It has been indeed proposed, on the basis of $^1$H NMR data, that some organized structure was detectable in the regions including the Trp residues in both peptides, i.e., the N-terminus of ACTH(1–24) and the 22–25 region of glucagon (Boesch et al., 1978; Toma et al., 1981). The existence of such structures has been first suggested by Eisinger (1969) in ACTH(1–24) by Tyr-2–Trp-9 energy-transfer studies. Moreover, the flexibility of the C-terminus has been underlined by Schiller (1972) in Trp-9–dansyllysine-21 energy-transfer studies. Owing to the existence of these substructures in aqueous solutions and to the fast internal motion of the Trp residue, the fluorophore is able to sample many local side-chain and solvent interactions during the excited-state lifetime.

*Heterogeneity of the Trp Environment in Reverse Micelles.* Incorporation of the peptides and of NATA into reverse micelles leads to a blue shift of the emission maximum as compared to water solutions. Two sets of situations are met according to the peptide net charge as a function of the micellar water content. The basic peptide ACTH(1–24)—bearing the highly charged sequence Lys-15-Lys-16-Arg-17-Arg-18 and the basic amino acid residues Arg-8, Lys-11, and Lys-21—does not display any further variation of its maximum fluorescence emission wavelength in the $w_0$ range between 7 and 22.4, where the amount of mobile water molecules increases (Thompson & Gierash, 1984). The neutral peptides, ACTH(5–10), glucagon, and NATA, exhibit an enhanced blue shift, in correlation with the decrease of the micellar water content in the same range of $w_0$. Since in all the studied peptides the Trp residues remain susceptible to a large extent to oxidation by *N*-bromosuccinimide, an interpretation of the spectral blue shift in terms of water solvent relaxation seems to be relevant. Such a mechanism can also explain the subsequent blue shift observed at $w_0 < 7$, where the surfactant sulfonate groups are not yet fully hydrated (Wong et al., 1976; Maitra, 1984; Thompson & Gierash, 1984). Excited-state fluorescence lifetime measurements for both ACTH(1–24) and glucagon are in agreement with the solvent relaxation process since the amplitudes of both time components calculated from a biexponential fit of the data remain unchanged as a function of the emission wavelength. Moreover, it is worthwhile to remark that only for glucagon the increase of the mean excited state lifetime is more important at high micellar water content, whereas for ACTH(1–24) it stays unaffected by it. From these observations, a model for the respective location of the Trp residues within the micelle can be proposed: owing to strong electrostatic interactions between the positively charged ACTH(1–24) and the AOT sulfonate groups, the Trp-9 residue is likely to be maintained in the strongly immobilized water shell. In contrast, the Trp residues in the uncharged peptides ACTH(5–10) and glucagon are probably located close to the center of the micelle where the mobile water molecules provide a more relaxed solvent environment.

The case of the model compound NATA is worthwhile to consider in detail. Non-monoexponential fluorescence total intensity decays are observed in reverse micelles, in contrast to bulk water. Emission wavelength dependence of the total fluorescence decay parameters evidences two situations according to the micellar water content. At high $w_0$ values, the data suggest the existence of two major populations of emitting species in these micelles: a first one in the more mobile water next to the center of the micelle and a second one in the highly immobilized water close to the surfactant sulfonate groups. In contrast, at low $w_0$ values, the results can be interpreted as arising from a solvent relaxation effect, as observed in glycerol solutions of high viscosity (Lakowicz & Cherek, 1980).

In addition, all the peptides and NATA as well exhibit a shorter mean excited-state lifetime in reverse micelles of high $w_0$ than in bulk water in relation with their possible location in the micellar water pool. As it has been suggested by Wahl and co-workers in their studies of dioxane–water solutions of indole derivatives (Privat et al., 1979), a modification of the hydrogen bonds between the indole and the structured water as compared to bulk water can explain in part the above observations.

*Trp Internal Dynamics and Overall Peptide Rotational Diffusion in Reverse Micelles.* Upon transfer of the peptides from aqueous solutions into reverse micelles a severe slowing down of the peptide internal dynamics and a strong limitation of the restricted angle of rotation are observed at the Trp level. The amplitude of these effects is more important when the Trp residue is close to the surfactant–water interface like Trp-9 in ACTH(1–24). Besides, the existence of a residual very fast restricted internal rotation is suggested from the low value of the initial anisotropy at zero time of the decays. Fast and slow internal Trp motions can be tentatively related to two modes of rotation (in- and out-of-plane) of the indole ring (Weber, 1971).

The overall tumbling of all peptides is slowed down in reverse micelles as compared to water. The amplitude of this effect is a function of the micellar water content and of the peptide charge. For the overall rotational motion of a rigid body entrapped in reverse micelles, two limiting cases can be considered according to their size (Keh & Valeur, 1981). At low $w_0$ values, corresponding to small-size micelles, the microscopic viscosity is considerably higher than that in bulk water (Tsuji et al., 1983). The solute is not allowed to rotate freely within the micelle, and the long correlation time of the anisotropy decay corresponds to the rotational diffusion of the micelle itself. At high $w_0$ values, the rotational correlation time of the micelle is larger since its volume increases (Chatenay et al., 1985). However, the microscopic viscosity inside the micelle decreases, and therefore, the tumbling of the solute within the micellar water pool starts to occur. In this case, the long correlation time is a combination of both rotational processes: the rotational diffusion of the peptide within the micelle and the rotational diffusion of the micelle itself.

The strength of coupling between the two rotational motions is governed not only by the interactions between the solute and the surfactant but also by interactions with the embedded water. In this respect, ACTH(1–24) interacts more strongly than glucagon and ACTH(5–10) with the AOT sulfonate groups and displays a stronger coupling. The influence of the peptide–water interactions on the coupling mechanism is suggested by the fact that despite their differences in molecular weight ACTH(5–10) and glucagon display a similar overall tumbling at high $w_0$ values.

*Conformational Changes in Reverse Micelles.* While glucagon monomers exhibit large amounts of extended, flexible structure in dilute aqueous solutions, the incorporation of the hormone in reverse micelles induces a significant amount of $\alpha$-helix. A very similar result has been reported by Braun et al. (1983). Using high-resolution $^1$H NMR, they have demonstrated that the binding of glucagon to dodecylphosphocholine micelles results in the folding of three turns of an irregular $\alpha$-helix in the 17–29 region of the peptide.

Another significant result is that the folded structure of glucagon is unaffected by the amount of water present, in the 3.5–22.4 $w_0$ range. This can be explained by the relative few intramolecular hydrogen bonds found by Braun et al. (1983) in the 17–29 C-terminal region. According to these authors, the same residues are also involved in a hydrophobic cluster comprising side chains of Ala-19, Phe-22, Val-23, Trp-25, and Leu-26. The $\alpha$-helices including these residues seem therefore less prone to be disrupted by additional free water. Furthermore, hydrogen bonds between the surfactant polar head groups and the peptide backbone may stabilize the folded structure.

ACTH(1–24) also displays a more ordered conformation when transferred from aqueous to reverse micellar solutions. In the latter case electrostatic interactions must occur between the positively charged side chains of Lys-15-Lys-16-Arg-17-Arg-18, to a lesser extent of Arg-8 and Lys-11, and between the negatively charged sulfonate groups of the surfactant. As a consequence, a restricted internal mobility is observed (see Fluorescence Anisotropy).

When ACTH(1–24) is inserted into the lipid phase (Gremlich et al., 1983), the 1–10 N-terminal peptide adopts an $\alpha$-helical structure while, when incorporated into reverse micelles, we observe the predominance of a $\beta$-pleated sheet. The occurrence of a rigid, antiparallel $\beta$-sheet has been observed by these authors with a synthetic ACTH(1–10) fragment in dry films or dry lipid multilayers and was immediately disrupted by hydration. In reverse micelles, the folding of the hormone is also dramatically affected by the presence of increasing amounts of water, since the interactions with the water dipoles become prominent and, as a consequence, most of the $\beta$-structure is disrupted. This effect may be also due to the weakening of the interactions between the sulfonate groups and the side chains responsible for the formation of $\beta$-structures. Under such circumstances, Trp-9 still remains in the close neighborhood of the water–surfactant interface because of the vicinity of charged Arg-8 and Lys-11, as made evident earlier in this paper by fluorescence measurements.

## Conclusions

In this work, we have extended to peptide hormones our earlier studies on a peripheral membrane protein, the myelin basic protein (Nicot et al., 1985). We have shown that the electrostatic interactions of the side chains, the hydrogen bonding with the surfactant polar head groups as well as with water, are crucial for the localization and the conformational distribution of ACTH(1–24) and glucagon with respect to the micellar interface. The biological relevance of these results may thus pertain to the mechanisms by which interactions with membrane surfaces select preferred conformations and orientations of biologically active peptides or proteins in recognition processes (Sargent & Schwyzer, 1986).

## Acknowledgments

J.G. and M.V. thank J. C. Brochon from LURE (CNRS, Orsay) for helpful discussions and for the facilities in using the time-resolved fluorescence setup of ACO. J.G. and M.V. are also indebted to the technical staffs of LURE and LAL laboratories for running the synchrotron radiation facilities. M.W. and C.N. are grateful to Dr. Garnier-Sullerot for the use of her J. Y. Mark V spectropolarimeter and to Dr. P. Kahn for stimulating discussions. We gratefully acknowledge the excellent editorial work of M. Rogard.

**Registry No.** Trp, 73-22-3; ACTH(1–24), 16960-16-0; ACTH(5–10), 4086-29-7; glucagon, 16941-32-5.

## References

Berlman, I. B. (1971) in *Handbook of Fluorescence Spectra of Aromatic Molecules*, 2nd ed., p 220, Academic, New York and London.

Birch, D. J. S., & Inhof, R. E. (1981) *Rev. Sci. Instrum. 52*, 1206–1212.

Blundell, T., & Wood, S. (1982) *Annu. Rev. Biochem. 51*, 123–154.

Boesch, C., Bundi, A., Oppliger, M., & Wuthrich, K. (1978) *Eur. J. Biochem. 91*, 204–214.

Bornet, H., & Edelhoch, H. (1971) *J. Biol. Chem. 246*, 1785–1792.

Braun, W., Wider, G., Lee, K. H., & Wuthrich, K. (1983) *J. Mol. Biol. 169*, 921–948.

Brochon, J. C. (1980) in *Protein Dynamics and Energy Transduction* (Ishiwata, S., Ed.) Proceedings of the 6th Taniguchi International Symposium, Biophysics Division, Tokyo, pp 163–169, The Taniguchi Foundation, Tokyo.

Chatenay, D., Urbach, W., Cazabat, A. M., Vacher, M., & Waks, M. (1985) *Biophys. J. 48*, 893–898.

Chatenay, D., Urbach, W., Nicot, C., Vacher, M., & Waks, M. (1987) *J. Phys. Chem. 91*, 2198–2201.

Cockle, S. A., & Szabo, A. G. (1981) *Photochem. Photobiol. 34*, 23–27.

Deber, C. M., Behnam, B. A. (1985) *Biopolymers 24*, 105–116.

Deranleau, D. A., Ross, J. B. A., Rousslang, K. W., & Kwiram, A. L. (1978) *J. Am. Chem. Soc. 100*, 1913–1917.

Eisinger, J. (1969) *Biochemistry 8*, 3902–3908.

Epand, R. M., & Surewicz, W. K. (1984) *Can. J. Biochem. 11*, 1167–1173.

Gottlieb, Y. Ya., & Wahl, Ph. (1963) *J. Chim. Phys. 60*, 849–856.

Gratzer, W. B., Beaven, G. H., Rattle, H. W. E., & Bradbury, E. M. (1968) *Eur. J. Biochem. 3*, 276–283.

Greff, D., Toma, F., Fermandjan, S., Löw, M., & Kisfaludy, L. (1976) *Biochim. Biophys. Acta 439*, 219–231.

Gremlich, H. U., Fringeli, P., & Schwyzer, R. (1983) *Biochemistry 22*, 4257–4264.

Grinvald, A., & Steinberg, I. Z. (1974) *Anal. Biochem. 59*, 583–598.

Grinvald, A., & Steinberg, I. Z. (1976) *Biochim. Biophys. Acta 427*, 663–678.

Inokuti, M., & Hirayama, F. (1965) *J. Chem. Phys. 43*, 1978–1989.

Jameson, D. M., & Alpert, B. (1979) in *Synchrotron Radiation Applied to Biophysical and Biochemical Research*

(Castellman, A., & Quercia, I. F., Eds.) pp 183–201, Plenum, New York.
Kaiser, E. T., & Kezdy, J. F. (1983) *Proc. Natl. Acad. Sci. U.S.A. 80*, 1137–1143.
Keh, E., & Valeur, B. (1981) *J. Colloid Interface Sci. 79*, 465–478.
Kinosita, K., Kawato, S., & Ikegami, A. (1977) *Biophys. J. 20*, 289–305.
Lakowicz, J. R., & Cherek, H. (1980) *J. Biol. Chem. 255*, 831–834.
Lakowicz, J. R., Maliwal, B. P., Cherek, H., & Balter, A. (1983) *Biochemistry 22*, 1741–1752.
Lipari, G., & Szabo, A. (1980) *Biophys. J. 30*, 489–506.
Luisi, P. L., & Magid, L. J. (1986) *Crit. Rev. Biochem. 20*, 409–474.
Luisi, P. L., Meier, P., Imre, V. E., & Pande, A. (1984) in *Reverse Micelles* (Luisi, P. L., & Straub, B. E., Eds.) pp 323–337, Plenum, New York.
Maitra, A. (1984) *J. Phys. Chem. 28*, 5122–5125.
Merola, F., & Brochon, J. C. (1986) *Eur. J. Biophys. 13*, 291–300.
Nabedryk-Viala, E., Thiery, C., Calvet, P., Fermandjan, S., Kisfaludy, L., & Thiery, J. M. (1978) *Biochim. Biophys. Acta 536*, 252–262.
Nicot, C., Vacher, M., Vincent, M., Gallay, J., & Waks, M. (1985) *Biochemistry 24*, 7024–7032.
Privat, J. P., Wahl, Ph., & Auchet, J. C. (1979) *Biophys. Chem. 9*, 223–233.
Ross, J. B. A., Rousslang, K. W., & Brand, L. (1981) *Biochemistry 20*, 4361–4369.
Sargent, D. F., & Schwyzer, R. (1986) *Proc. Natl. Acad. Sci. U.S.A. 83*, 5774–5778.
Schiller, P. W. (1972) *Proc. Natl. Acad. Sci. U.S.A. 69*, 975–979.
Schiller, P. W. (1985) in *The Peptides* (Hruby, V. J., Ed.) pp 115–164, Academic, New York.
Schneider, A. B., & Edelhoch, H. (1972) *J. Biol. Chem. 247*, 4986–4991.
Schulster, D., & Schwyzer, R. (1980) in *Cellular Receptors for Hormones and Neurotransmitters* (Schulster, D., & Levitski, A., Eds.) pp 197–217, Wiley, New York.
Spande, T. F., & Witkop, B. (1967) *Methods Enzymol. 11*, 498–506.
Spencer, R. D., & Weber, G. (1970) *J. Chem. Phys. 52*, 1654–1663.
Thompson, F., & Gierash, L. M. (1984) *J. Am. Chem. Soc. 106*, 3648–3652.
Toma, F., Fermandjian, S., Low, M., & Kisfaluby, L. (1981) *Biopolymers 20*, 901–913.
Toma, F., Dive, V., Low, M., & Kisfaluby, L. (1985) *Prog. Bioorg. Chem. Biophys. 2*, 125–133.
Tran, C. D., Beddard, G. S., & Osborne, A. D. (1982) *Biochim. Biophys. Acta 709*, 256–264.
Tsuji, K., Sunamoto, J., & Fendler, J. H. (1983) *Bull. Chem. Soc. Jpn. 56*, 2889–2893.
Valeur, B., & Weber, G. (1977) *Photochem. Photobiol. 25*, 441–444.
Vincent, M., Gallay, J., De Bony, J., & Tocanne, J. F. (1985) *Eur. J. Biochem. 150*, 341–347.
Wahl, Ph. (1975) in *New Techniques in Biopolymers and Cell Biology* (Pain, H., & Smith, B., Eds.) Vol. 2, pp 233–285, Wiley, London.
Wahl, Ph. (1979) *Biophys. Chem. 10*, 91–104.
Wahl, Ph., Auchet, J. C., & Donzel, B. (1974) *Rev. Sci. Instrum. 45*, 28–32.
Wallach, D. (1967) *J. Chem. Phys. 47*, 5258–5268.
Weber, G. (1971) *J. Chem. Phys. 55*, 2399–2407.
Wong, M., Thomas, J. K., & Gratzel, M. (1976) *J. Am. Chem. Soc. 98*, 2391–2397.
Woody, R. W. (1985) in *The Peptides* (Hruby, V. J., Ed.) pp 15–114, Academic, New York.
Yguerabide, J. (1972) *Methods Enzymol. 26*, 498–578.